

Water Self-Diffusion Coefficient Determination in an Ion Exchange Membrane by Optical Measurement

H. R. ZELSMANN* and M. PINERI, *Centre d'Etudes Nucléaires de Grenoble, Département de Recherche Fondamentale, Service de Physique, Groupe Physico-Chimie Moléculaire, 85 X-38041 Grenoble Cedex, France*, and M. THOMAS and M. ESCOUBES, *Université Claude Bernard Lyon I, U.A. 507, 43 bd du 11 Novembre 1918, 69622 Villeurbanne Cedex, France*

Synopsis

The self-diffusion coefficient of water in a perfluorinated ionic membrane has been measured for different water contents corresponding to water vapor pressures less than the saturated one. The isotope method usually employed in the liquid state was extended to vapors, which led us to an observation of three different isotopic species by quantitative far IR spectroscopy. Two measurement methods are presented permitting a determination of the time lag and hence of the diffusion coefficient. The slow variation of the diffusion coefficient with the water concentration, as well as the good agreement of the numerical results given by different methods (permeation-sorption) are explained by the fact that no plasticization occurs. This result has been independently verified by other experiments.

INTRODUCTION

The transport properties of a dense perfluorinated ionic Nafion (DuPont) membrane for water have been investigated within a larger project¹ with respect to the following:

1. Direct determination of the different transport parameters such as the coefficients of solubility, permeability, diffusion, and the concentration profiles during gas permeation
2. Evolution of these parameters with the permeation conditions on the upstream and downstream sides
3. Definition of the relation between the molecular structure² of the membrane and the above-mentioned parameters.

The work presented here is more closely related to the determination of the coefficient of self-diffusion for water concentrations smaller than the water content of the membrane in saturated conditions. The usual methods for measuring such a diffusion coefficient D are based on sorption techniques (determination of the kinetics) and on permeation techniques (observation of a time lag). However, both of them are not independent of the mass transport. The

* Université Joseph Fourier de Grenoble.

coefficient of self-diffusion D^* is the limit of the diffusion coefficient at zero mass transport. By using isotopically different molecules and by tracing them, it is possible to measure this coefficient D^* directly.

When the diffusion is independent of permanent concentration, the two diffusion coefficients are related by³

$$D^* = \frac{D}{1 - \varphi} \frac{\partial \ln c}{\partial \ln a} \quad (1)$$

where a is activity, c is concentration and φ is the fractional volume. In systems where there is no difference between concentration and activity, and for sufficiently small volume fractions, the two coefficients become equal.

Let us comment first on the diffusion coefficient determination by the sorption and permeation measurements. In the case of diffusion that is governed by Fick's law, the sorption ratio α is proportional to the square root of time as long as $\alpha \leq 0.5$. Under these conditions we may deduce the diffusion coefficient D for a given membrane thickness e^4 from

$$\alpha = \frac{4}{\sqrt{\pi}} \left(D \frac{t}{e^2} \right)^{1/2} \quad (2)$$

and for $\alpha = 0.5$ at half-sorption ($t_{1/2}$):

$$D = \frac{0.049e^2}{t_{1/2}} \quad (3)$$

This relation results from the superposition of the two fluxes established between each membrane surface and the median plane, supposing the median plane is at zero concentration. It assumes that the permeating molecules do not reach the center of the membrane for a large fraction of the sorption.

The diffusion coefficient D can also be obtained from permeation measurements. With this assumption that Fick's law is valid, the quantity Q of the molecules having diffused at a time t through the membrane⁵⁻⁸ may be expressed by

$$Q = \frac{Dc_1}{e} \left(t - \frac{e^2}{6D} \right) \quad (4)$$

c_1 here is the equilibrium concentration of sorption on the upstream interface; the concentration on the downstream interface is maintained at a value close to zero. A plot of Q versus t defines the time lag θ by the position of the intersection with time axis, and D can be obtained from this value θ by

$$D = \frac{e^2}{6\theta} \quad (5)$$

There are strong limitations in these two experimental determinations of D . These two experiments give a diffusion coefficient averaged over different

permanent concentrations in the membrane. The aim of this article is to propose a technique based on optical analysis for measuring D inside the membrane under uniform conditions of water content throughout the whole membrane.

OPTICALLY DETECTED DIFFUSION

Principle of Isotope Tracing with HHO/DDO

The major idea of this method is to start with an equilibrium state of the membrane at a pressure p , between 0 and 17 torr, with DDO on both sides of the membrane. At the beginning of the diffusion process DDO is replaced on the one side by HHO at the same pressure. As the diffusion goes on, one may observe increasing amounts of the HDO molecule on either side of the membrane by spectroscopical analysis. Equations (4) and (5) may apply to the labeled water molecule with the concentrations c being the equilibrium concentration at the beginning of the experiment.

Due to its high sensitivity, infrared spectroscopy is one of the most powerful qualitative and quantitative methods for the detection of the isotopic species of water. Technological considerations may perhaps favor the choice of mid-IR; the far-IR, however, has the advantage of a very low detection limit for water. Another and not less important advantage of FIR is that the resolving power can be at least 20 times lower than for mid-IR at equal linewidth. From the theoretical point of view a pure rotational spectrum of water vapor, even if it is very complex, will necessarily be simpler than a mid-IR vibration-rotation spectrum. For these reasons we choose FIR spectroscopy as the analytical tool for our experiment.

Experimental

Spectrometer

The water vapor spectra were recorded on a POLYTEC FIR30 interferometer between 20 and 250 cm^{-1} . As the interferometer was operated under a vacuum of typically 10^{-2} torr (thus the gas cell in the sample compartment was surrounded by vacuum too), no water vapor contribution could be detected other than the one in which we were interested.

The source aperture was chosen to be 3 mm, and all spectra were run with a nonapodized resolution of 0.15 cm^{-1} in order to clearly discern the lines associated with the different species present. Our FIR detection system consisted of a Ge-bolometer operated at 4.2 K (from Infrared Laboratories) with a NEP of 6×10^{-13} W/Hz^{1/2} and a lock-in amplifier PAR 5209 with a PAR 196 light chopper.

The control of the interferometer, data acquisition, and data processing were performed by a Hewlett-Packard series 217 workstation. The programming facilities of this scientific computer turned out to be very well suited for the specific tasks of this type of experiment.

Diffusion Circuit and Its Operation

In Figure 1 we show the experimental setup for the diffusion experiment. It consists of two constant-temperature baths, containing a glass bulb with de-

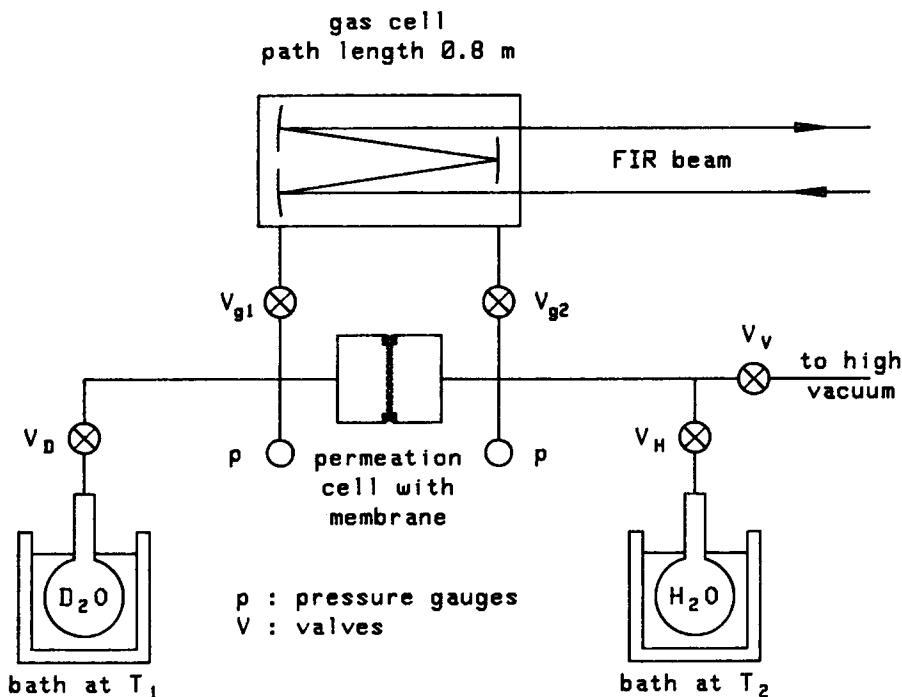


Fig. 1. Experimental setup showing the principal elements for the diffusion experiment.

gassed light and heavy water, respectively, a cell with a Nafion membrane of about 35 cm^2 , two Barocel 600 pressure sensors from Datametrics, a custom-built multiple-pass White cell (with a path length adjustable from 0.8 to 4.8 m), and a high-vacuum pump. All parts in contact with water vapor were made of stainless steel in order to limit possible artifacts of adsorption or desorption during the experiment.

The first step of operation is to evacuate all atmospheric humidity from the system and to allow desorption of all surfaces as well as possible. Depending on the preceding state, this may take a few hours. All valves are opened except those of the water bulbs.

In a second step the valve of the vacuum pump is shut off, and we admit to all the system D_2O vapor at a pressure that is defined by the temperature of the bath. As has been already shown,¹ it may take 2–3 h to get absorption equilibrium of the Nafion membrane.

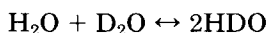
The third step marks the beginning of the diffusion process, which consists in closing valve V_{g2} and opening of valve V_H . Thus one admits ordinary H_2O vapor to the permeation cell at rigorously the same pressure. It should be noted here that the isotope effect of the water vapor pressure is far from being negligible,^{9,10} and a correct equilibrium pressure may be obtained by fixing the temperatures of the two independent baths accordingly. The control of the temperatures has to be better than $\pm 0.05^\circ\text{C}$.

The H_2O molecules begin to diffuse through the membrane and will get into the gas cell after a characteristic time delay. The FIR spectra show the rise of the typical H_2O absorption lines as time and diffusion progress.

Choice of the Experimental Conditions for Diffusion

The performance of this type of measurement has been tested in a series of preliminary runs for water vapor pressures ranging from 0.1 to 5 torr for the two isotopic species. We found that the relation between absorbance and pressure was linear, as it should be. Saturation of the most intense lines could be avoided or at least limited by an appropriate choice of the path length of the cell, which was generally 0.80 m. All tests on leakage and desorption from surfaces were very satisfactory. A final verification in this context was the analysis of a mixture containing 1% D₂O in H₂O, which showed that minor isotopic impurities could be quantified in good conditions.

For any mixture of H₂O and D₂O we have to consider the equilibrium of the reaction



with a disproportionation constant $K_c = 3.74$ at 0°C.¹⁰ In the case of an initial content of 1% D₂O we get 1.98% of HDO as the equilibrium establishes on the side of HDO. The pure D₂O whose concentration is 0.01% becomes undetectable.

For our diffusion experiment we had to choose the fully deuterated water as the initial state and to monitor the small quantities of light water, which convert into HDO molecules. The reason for this choice becomes evident when looking at the empirical formula defining the logarithm of the ratio of pressures as a function of absolute temperature (valid for liquid H₂O and D₂O in a temperature range of $268 < t < 353$ K),¹⁰:

$$\ln p(\text{H}_2\text{O})/p(\text{D}_2\text{O}) = 0.202524 - 209.412/T + 57320.6T^2 \quad (6)$$

This shows us that the water vapor pressure for H₂O is always higher than that of D₂O. For the lowest temperatures this amounts to 20% difference. Therefore, if starting from H₂O at pressures close to saturated ones, it would be impossible to replace the H₂O molecules by D₂O molecules at the same pressure because condensation occurs.

Spectrometric Detection

First Method: Observation of Resolved Lines

The first method of analysis consisted of the measurement of some selected HDO lines that were clearly resolved and not mixed or overlapped by D₂O lines. This statement may seem obvious from the theoretical point of view, but a closer look reveals an extremely "rich" spectrum with only a few good candidates for correct evaluation. In fact, there are some 900 observable absorption lines in the far infrared corresponding to pure rotational transitions in the vibrational ground state for a mixture of H₂O, HDO, and D₂O.

The rotational lines of ordinary water are actually known to a very high degree of accuracy as to their positions, but to a lesser degree for their absolute intensities. The most important compilations in this field, the *HITRAN Molecular Database* (1986 edition) from the U. S. Air Force Geophysics Laboratory¹¹ or the data collection from Guelachvili and Rao¹² may serve to trace the

H₂O lines. For the HDO lines, however, the information is much less complete, as the natural abundance for HDO is relatively low. Finally for the heavy-water molecule only scarce data of direct observation is available at all, coming essentially from microwave experiments.

In order to solve the problem of identification of the different water lines, we took the respective energy levels and recalculated the line positions for a set of about 70 of the most intense lines of the three species. The energy level data were taken from Flaud et al.¹³ for H₂O, from Messer et al.¹⁴ for HDO, and from Papineau et al.¹⁵ for D₂O. By this procedure we were able to assign about 20 nonidentified lines of HDO to low-order quantum number transitions in Ref. 12.

Simultaneously we got a confidence check for the calibration of our interferometer that showed us that the positions of isolated lines were correct to $\pm 0.001 \text{ cm}^{-1}$.

For the numerical analysis we retained a set of 24 HDO lines and 7 H₂O lines from which we got either the absorbance readings or an integrated absorbance value. The acquisition of one full resolution spectrum took about 30 min, so as diffusion progressed the H₂O and HDO lines became visible. A typical sequence of six spectra recorded at 7.35 torr is shown in Figure 2. The spectral interval of 105–110 cm^{-1} is one of the favorable regions without strong absorptions of D₂O, thus permitting confident integration of the absorbance. The interesting quantities, the absorptions of HDO and H₂O, may be obtained directly by recording the reference spectrum prior to the start of diffusion. The absorptions of the D₂O molecule, however, cancel very well as long as the lines do not saturate. The observed evolution of the diffusion process on a time scale is represented in Figure 3, where we show the integrated absorbance for five different spectral windows. As may be seen from this figure, the fitted curves

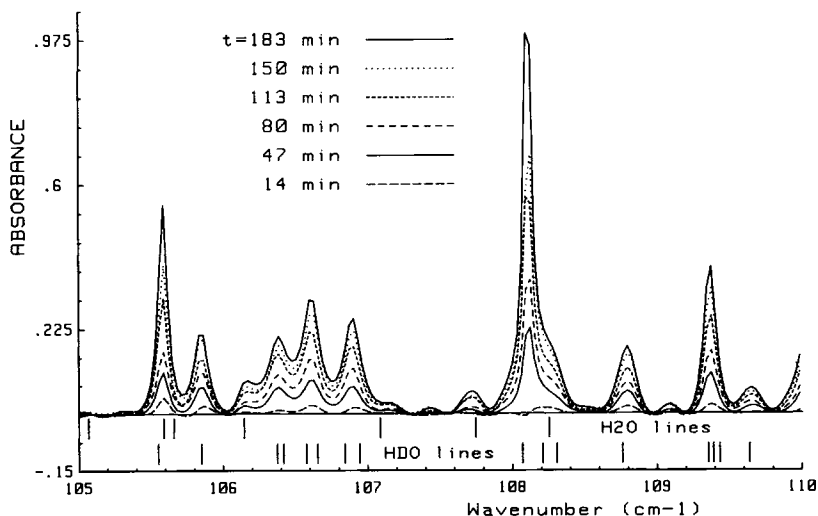


Fig. 2. Rotational water vapor spectra for six different diffusion times at a pressure of 7.35 torr. All ratios for the absorbance spectra are calculated with a background spectrum recorded prior to the beginning of diffusion at $t = 0$, so that the contributions of D₂O to the absorbance are canceled.

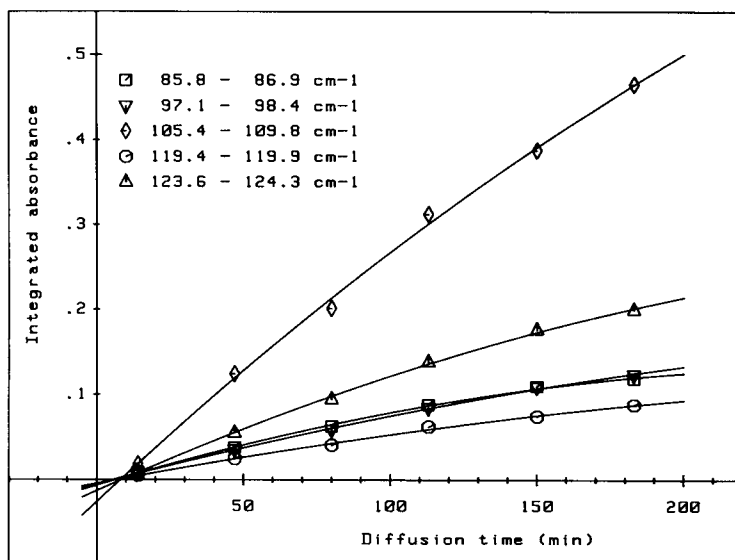


Fig. 3. Behavior of the integrated absorbance for five different spectral windows versus time. The experimental uncertainty is comparable with the symbol height.

intersect at a characteristic time, called the time lag, of the diffusion. From the slope of the curves we calculate the diffusion constant. Thus each spectrum of Figure 2 contributes to one abscissa point of the plot of the integrated absorbance versus time. For water vapor pressures higher than 5 torr we limited our observation time to about 3 h as some HDO lines tended to saturate.

Second Method: Observation of Integrated Intensity

In spite of its straightforward data processing application, the first method was not satisfactory for getting values of the time lag on a time scale of several minutes. The time to acquire a whole spectrum was so long that we had to find a method of direct observation of the evolution of the absorbance with time. With an interferometer it is not possible (due to its physical principle) to monitor a spectral intensity at a fixed wavenumber, as can be done with a dispersive instrument. However, this problem may be solved in an elegant and unusual way. A look at the expression for the luminous intensity $I(\delta)$, which reaches the detector of an interferometer, may show with more clarity the difference between the two methods. It is given by

$$I(\delta) = \int_{-\infty}^{\infty} L(\tilde{\nu}) [1 + \cos(2\pi\delta\tilde{\nu})] d\tilde{\nu} = I_0 + I_{fg}(\delta) \quad (7)$$

The optical path difference in centimeters is noted by δ , the wavenumber $\tilde{\nu}$ is in cm^{-1} , and $L(\tilde{\nu})$ is the distribution function of amplitudes over the total spectral window or simply the "spectrum." As one can see, the observed signal is split into two parts:

1. Part I_0 is independent of the path difference (or the mean intensity of the interferogram) and presents in the space of wavenumbers the total (or integrated) intensity of the spectrum.
2. A periodically modulated part that depends on the path difference, generally called interferogram function $I_{fg}(\delta)$, and that is the Fourier transform of $L(\tilde{\nu})$. We should add here that this modulation is an intrinsic property of an interferogram and should not be confused with any modulation that is needed for signal processing.

For the normal spectral analysis, as we did by the first method, one drops the term I_0 (if it has not yet been done automatically by the fast scanning interferometer), and the spectrum is calculated from the interferogram function $I_{fg}(\delta)$.

With a slow scanning interferometer it is possible to exploit the information content of I_0 . As the H_2O and HDO vapors show a lot of spectral absorption lines over the whole far infrared region, it is possible to measure the intensity integrated over all wavenumbers falling onto the detector as a function of diffusion time directly. The sampling is no longer controlled by an incremental measurement system for the path difference, but rather by the clock of the computer. With the mobile mirror of the interferometer held in a fixed position ($\delta = \text{constant}$), we recorded the drop of intensity due to the increasing number of molecules having diffused at time intervals of 1 or 2 s. Theoretically the value of the chosen path difference does not matter, but it is better to take a value a few centimeters apart from the central fringe, in order to get readings that are less subject to perturbations. A typical recording of the total spectral intensity by this method is shown in Figure 4. Apart from some fluctuations

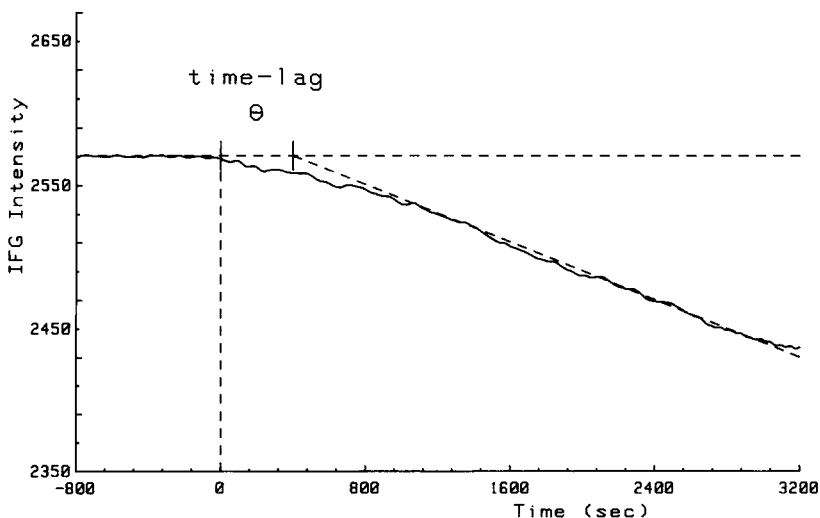


Fig. 4. Measurement of the time lag by the second method (see text). The represented quantity is the intensity of the interferogram at a fixed path difference, which is identical to the observed total spectral intensity. The run shown here was for a pressure of 12 torr measured at time intervals of 2 s.

due to noise, the observed intensity remains constant for times prior to the beginning of diffusion. Once the diffusion is started, there is a characteristic time lag θ before the intensity falls. This decreasing intensity can be assumed to be linear as long as a series development is justified by the absolute magnitudes. We should give here some indications about the stability of our interferometer. The stability on a time scale of a few minutes is shown by the irregularities of the curve in Figure 4, whereas drift over 24 h is typically within 1% of absolute intensity.

There are some major advantages to this procedure. First, time lags with values on the order of a few minutes can be evaluated correctly in contrast to the first method. Second, the exploitation does not need high-resolution spectra with tedious identification of spectral lines, and it is thus much simpler. As the calculation of the diffusion coefficient is done by the relation of Eq. (5), it is not necessary to establish any calibration curve, for we need only the value of the starting point of the total spectral intensity.

RESULTS AND DISCUSSION

A summary of our results is given in Figure 5, where we compare the diffusion coefficients determined by different experimental methods and for different relative water pressures. The three methods that give us a diffusion coefficient for water in the liquid state follow:

1. The technique of self-diffusion with tritium-labeled liquid water that can be traced by radioactive analysis
2. The technique of pervaporation using liquid water on the upstream side
3. The technique of sorption and recording the dimensional changes of the membrane soaked in water.

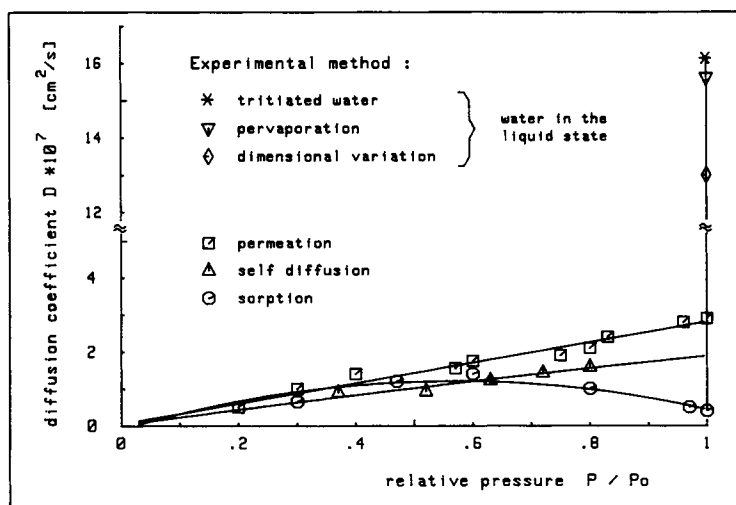


Fig. 5. Water diffusion coefficients for different relative pressures and for the liquid state in a Nafion membrane. The uncertainty of the data is within the symbol size. For the liquid state data it is slightly greater (note the change of scale).

The numerical values for the diffusion coefficient are rather similar: their average is about $1.5 \times 10^{-6} \text{ cm}^2/\text{s}$.

As may be seen in Figure 5, the coefficients for water in the gas state show a similar tendency and similar absolute values for D , which range between 1 and $3 \cdot 10^{-7} \text{ cm}^2/\text{s}$. The decrease observed with the sorption technique is discussed in more detail below.

Concerning the self-diffusion experiment with water in the gas state, it should be noted that the measurements extend only up to a relative pressure of 0.8. This is due to the vapor pressure isotope effect of water, which does not allow an experiment with a higher fraction of the saturated pressure. A systematic comparison of the two methods of measurement and analysis employed with the spectrometric detection of self-diffusion gave us very similar values for D^* and were reproducible within $\pm 5\%$.

In order to explain these observed diffusion coefficients we have to discuss several hypotheses. Let us first look at the effect of plasticization of the membrane. The relation between diffusion coefficient and plasticization coefficient is given by the classical expression

$$D = D_0 \exp(\gamma C) \quad (8)$$

This clearly means that plasticization effects and concentration profiles are directly connected; the larger γ is, the more convex on the downstream side is the profile. As we have already emphasized, the self-diffusion conditions imply a constant concentration profile across the membrane, which is not the case in permeation or sorption conditions. A comparison of the results obtained by the different techniques shows us that to a first approximation the diffusion coefficients do not depend on the concentration profile. As this condition is only verified for a γ close or equal to zero, we may consequently rule out an effect of plasticization. We underline the difference with irradiation-grafted membranes,¹⁶ where changes in D of several orders of magnitude have been measured and values between 10 and 100 have been calculated.

From the present results we expect a quasi-linear profile for water permeation through the Nafion membrane. Experimental evidence of such linear profiles has recently been given by small-angle neutron scattering.¹⁷

Since plasticization does not explain our results, we have to find another reason to understand the small increase of the diffusion coefficients with the relative pressure up to 0.7 and the drastic change observed between the gas and liquid conditions. An interpretation, consistent with the other transport properties obtained from other experiments,¹ is associated with the changes of structure that occur upon hydration. At low water contents corresponding to low water pressures, the water-swollen ionic domains are separated by an organic matrix that limits the diffusion. A small increase of the diffusion coefficient is observed due to the increase of the volume fraction of these hydrophilic domains. When soaking in water the swelling is large enough to permit the percolation of the ionic domains, and the measured diffusion coefficient is associated with this water containing phase.

The lower values of the diffusion coefficients measured in sorption are sometimes interpreted to be due to a decrease in the water concentration gradient between the center of the membrane and the two external faces. This effect is

generally important for thin membranes with high plasticization coefficients. Such an explanation cannot apply in our case. The kinetic differences observed close to the saturated pressure between sorption and permeation measurements may be due to a slowing down of surface adsorption. For relative water pressures larger than 0.7, the surface equilibria do not establish instantaneously; this is thus a limiting step for sorption, whereas in permeation and self-diffusion this problem does not exist. In permeation the flux establishes without equilibrium on the upstream side. For self-diffusion, the equilibrium is established before the measurement. Finally, for liquid water conditions, such a limitation is not observed because in this case we have much higher molecule concentration at the interface.

This hypothesis has been verified from the small-angle neutron scattering measurements of the concentration profiles in permeation and pervaporation conditions.¹⁷ We have shown that the sorption equilibria are not obtained in permeation conditions for relative pressures larger than 0.7 while the water content corresponding to saturated conditions is obtained in pervaporation conditions.

These results have to be associated with other results concerning the interactions of water with ionic sites. Two different states for water absorption have been demonstrated from thermodynamic Mössbauer, electron spin resonance measurements. The first water molecules that are sorbed fill the first hydration shell of the cations, which occurs for relative water pressures close to 0.7. For the following water molecules there will be a much decreased interaction energy.

CONCLUSION

Self-diffusion coefficient measurements in membranes equilibrated at vapor pressures lower than saturated pressure have been made possible by using far infrared spectroscopy. Such an experiment is able to detect HDO concentrations lower than 0.01% in H₂O/D₂O vapor mixtures and, therefore, makes time-lag measurements possible. This type of analytical technique may be used with other membranes and other molecules in the gas state that show a dipole moment.

By comparison with the diffusion coefficients obtained from the classical sorption and permeation measurements, we can draw the following conclusions:

1. Changes in the water diffusion coefficients cannot be explained by plasticization of the Nafion by water but may be explained by structural changes that occur in the membrane upon water swelling.
2. Sorption experiments take into account the surface equilibria, which is neither the case for the self-diffusion experiments, in which the equilibrium is obtained before the measurement is made, nor for the permeation experiments where the water flux can be obtained without equilibrium conditions on the upstream side. If the surface adsorption processes are slower than the diffusion ones, the sorption kinetics can be very different from the two other experiments.

The above-mentioned results have been verified from the concentration profiles obtained from small-angle neutron scattering experiments in permeation or pervaporation conditions.

References

1. M. Thomas, M. Escoubes, M. Pineri, and H. R. Zelsmann, to appear.
2. E. J. Roche, M. Pineri, and P. Duplessix, *J. Polym. Sci. Polym. Phys.*, **20**, 481 (1982).
3. J. Crank, *The Mathematics of Diffusion*, Oxford University Press, London, 1970, p. 228.
4. J. Crank, G. S. Park, *Diffusion in Polymers*, Academic Press, New York, 1968, p. 2.
5. J. Comyn, *Polymer Permeability*, Elsevier Applied Science Publishers, London, 1985, p. 22.
6. A. Lejeune, Summer School on Membrane Science and Technology, Cadarache, 1984.
7. J. Crank, *The Mathematics of Diffusion*, Oxford University Press, London, 1970, pp. 5-7.
8. R. M. Felder, *J. Memb. Sci.*, **3**, 15 (1978).
9. J. Pupezin, G. Jakly, G. Jansco, and W. A. Van Hook, *J. Phys. Chem.*, **76**, 743 (1972).
10. G. Jansco and W. A. Van Hook, *Chem. Rev.*, **74**, 689 (1974).
11. A description of this database may be found in L. S. Rothman, R. R. Gamache, A. Barbe, A. Goldman, J. R. Gillis, L. R. Brown, R. A. Toth, J.-M. Flaud, and C. Camy-Peyret, *Appl. Opt.*, **22**, 2247 (1983), and references cited therein.
12. G. Guelachvili and K. N. Rao, *Handbook of Infrared Standards*, Academic Press, Orlando, 1986.
13. J.-M. Flaud and C. Camy-Peyret, *Molec. Phys.*, **26**, 811 (1973).
14. J. K. Messer, F. C. De Lucia, and P. Helminger, *J. Molec. Spectrosc.*, **105**, 139 (1984).
15. N. Papineau, J.-M. Flaud, and C. Camy-Peyret, *J. Molec. Spectrosc.*, **87**, 219 (1981).
16. R. Francois, "Thèse de Doctorat Institut National Polytechnique de Lorraine," Nancy (1988).
17. M. Thomas, M. Escoubes, P. Esnault, and M. Pineri, to appear.

Received April 3, 1989

Accepted November 20, 1989